First in Vivo SPECT Imaging of Mouse Femorotibial Cartilage Using 99mTc-NTP 15-5

Elisabeth Miot-Noirault, Aurélien Vidal, Philippe Auzeloux, Jean-Claude Madelmont, Jean Maublant, Nicole Moins

HAL Id: hal-01505259
https://uca.hal.science/hal-01505259

Submitted on 11 Apr 2017

First In Vivo SPECT Imaging of Mouse Femorotibial Cartilage Using ^{99m}Tc-NTP 15-5

Elisabeth Miot-Noirault, Aurélien Vidal, Philippe Auzeloux, Jean-Claude Madelmont, Jean Maublant, and Nicole Moins

Abstract

This study aimed to report the first single-photon emission computed tomographic (SPECT) imaging of articular cartilage in mice using ^{99m}Tc-NTP 15-5 radiotracer. Mice intravenously injected with ^{99m}Tc-NTP 15-5 were submitted to (1) dynamic planar imaging, (2) static planar imaging, (3) 1 mm pinhole SPECT acquisition, and (4) dissection. Tomographic reconstruction of SPECT data was performed with a three-dimensional ordered subset expectation maximization algorithm, and slices were reconstructed in three axes. ^{99m}Tc-NTP 15-5 rapidly accumulated in the joint, with a peak of radioactivity being reached from 5 minutes postinjection and maintained for at least 90 minutes. Given that bone and muscle did not show any accumulation of the tracer, highly contrasted joint imaging was obtained from 15 minutes postinjection. When 1 mm pinhole SPECT acquisition was focused on the knee, the medial and lateral compartments of both the femoral condyle and tibial plateau were highly delineated, allowing a separate quantitation of tracer accumulation within each component of the femorotibial joint. A good correlation was found between tracer uptake determined by region of interest analysis of both planar and SPECT scans and dissection. This new approach to imaging of cartilage in mice provides joint functionality assessment in vivo, giving a unique opportunity to achieve a greater understanding of cartilage physiology in health and disease.

O STEOARTHRITIS (OA) is the most common joint degenerative disease affecting around 10% of the world's population over the age of 60 years.[1] It is a slowly progressive pathology characterized by cartilage destruction leading to joint instability. As a consequence, there is a crucial need for both (1) targeted therapeutic strategies able to reduce or stop disease progression and (2) OA animal models for the preclinical validation of new disease-modifying osteoarthritis drugs (DMOADs) able to interact with the early molecular and biochemical pathways responsible for initiation and progression of disease.[2,3] The very early stages of OA are hallmarked by molecular and biochemical alteration of the extracellular matrix (ECM) of articular cartilage, that is, a loss of proteoglycans (PGs) and disruption of the collagen fibril network. The alteration of ECM integrity, mainly the loss of PG, is known to precede cartilage alteration and morphologic joint damages and has been considered to be one of the most appropriate targets for studying OA.[4–6] Recent advances in transgenic technologies have created great interest in controlled genetically engineered mice models, such as knockout mice with specific ECM mutations. Such models appear to be attractive for studying the role of ECM macromolecules in OA initiation and progression, as well as evaluation of the efficacy of these new emerging therapeutic strategies.[7–10] These OA experimental models offer many advantages, which can be summarized as follows: (1) pathologic OA pathways are as representative as possible of those described in humans, (2) the molecular etiology is known, and (3) the severity and progression of OA can be controlled to support the evaluation of new emerging therapies.[6–10] Biochemical and molecular mechanisms associated with OA development may be studied using specific markers and molecular probes able to identify altered cartilage ECM at different stages of disease progression. At present, the degree of severity of OA in mice is achieved by histologic examination, thus precluding any possibilities of

monitoring disease progression in serial studies in the same animals. The recent application of single-photon emission computed tomographic (SPECT) devices to small-animal imaging produces functional images at the millimeter scale and opens wide access to many human pathophysiology models at the molecular level.[11–15] Radionuclide imaging offers noninvasive and functional access to a specific biologic target in vivo, with a high sensitivity for deep tissue imaging and signal tissue quantitation. Scintigraphic techniques are able to detect very low concentrations of radiopharmaceuticals in vivo, with a selectivity that can be enhanced by vectorizing radiotracer to molecular or tissue targets. The vectorization toward cartilage matrix PGs is the strategy developed by and used in our group for many years. This strategy consists of using the quaternary ammonium function (that exhibits a high affinity for PG) as a selective carrier of oxotechnetium complex to cartilaginous tissues.[16,17,18] Technetium-99m N-[3-(triethylammonio)propyl]-15ane-N5 (^{99m}Tc-NTP 15-5) scintigraphic imaging was recently demonstrated to show a high sensitivity to enable accurate assessment of articular functionality in cartilage PG in two experimental OA models with markedly different etiopathologic factors.[18,19] On the basis of these encouraging results, we hypothesized that ^{99m}Tc-NTP 15-5 scintigraphic imaging would be a powerful tool to assess cartilage functionality in vivo in small animals, which has great potential for OA research.

In the present study, mice were intravenously (IV) injected with ^{99m}Tc-NTP 15-5 radiotracer and submitted to (1) dynamic planar imaging (DPI), (2) static planar imaging, (3) 1 mm pinhole SPECT acquisition, and (4) dissection. This article is the first to report SPECT imaging of articular cartilage in mice in vivo, providing a unique opportunity to achieve a greater understanding of cartilage physiology in health and disease.

Materials and Methods

Radiolabeled Tracer

The NTP 15-5 (Figure 1) was prepared and radiolabeled with ^{99m}Tc by the stannous chloride method as previously described.[17,18] Quality control was performed with Whatman Partisil KC18F strip thin layer chromatography using methanol:acetonitrile:tetrahydrofuran:ammonium acetate (1 N) (3:3:2:2) as eluent.
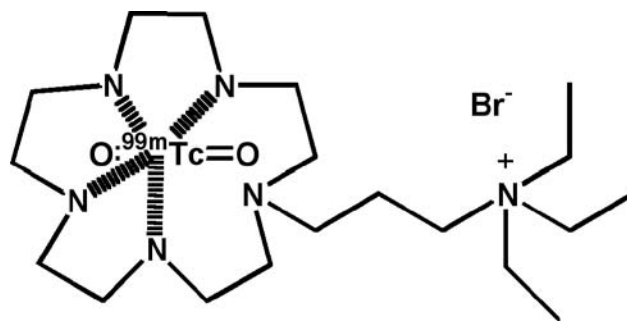

Figure 1. Chemical structure of technetium-99m N-[3-(triethylammonio)propyl]-15ane-N5 (^{99m}Tc-NTP 15-5).

Animals

Twenty-two male BALB/c mice, 6 weeks old and weighing about 25 g (Charles River, France), were used for the study. They were handled and cared for in accordance with the Guide for the Care and Use of Laboratory Animals (National Research Council, 1996) and European Directive EEC/86/809. Protocols were performed under the authorization of the French Direction des Services Vétérinaires (Authorization N° C63-113-10) and conducted under the supervision of authorized investigators in accordance with the institution's recommendations for the use of laboratory animals. For all imaging procedures, mice were anesthetized by intraperitoneal (IP) injection of 40 µL of a solution of ketamine (Imalgène 500, Rhone Mérieux, France) and xylazine (Rompun 2%, Bayer, France) (4:1).

Gamma Camera

Imaging was performed using a gamma camera dedicated to small-animal imaging (γIMAGER, Biospace Mesures, Paris, France) that allows planar and SPECT acquisitions. The gamma camera consists of a R 3292 Hamamatsu position-sensitive photomultiplier with a continuous 4 mm thick × 120 mm diameter CsI(Na) crystal leading to a 10 cm field of view. The energy resolution and intrinsic planar resolution of the basic system are given as 11% at 140 keV and < 2 mm full width at half maximum, respectively.

For planar imaging in mice, the camera was equipped with a 1.3/0.2/20 collimator (hole diameter/septum thickness/height in millimeters). For application to high-resolution SPECT imaging, the gamma camera was equipped with a pinhole collimator with a 1 mm aperture size. In this configuration, the detector was fixed and the animal was rotated,

with the rotation (1 turn/min) synchronized to data acquisition. The mechanical support was designed to have the midline of the sample exactly in the midline of the pinhole.

Distribution of ^{99m}Tc-NTP 15-5 Tracer IV Injected in Mice

Whole-Body DPI Study

First, DPI was performed (1) to visualize the kinetics of tracer distribution in the organs of interest and (2) to determine the optimal delay for SPECT acquisition. Anesthetized mice (*n* = 10) were positioned over the collimator of the gamma camera, with both femorotibial joints stretched in extension. Reproducibility in joint positioning for the serial images among all animals imaged was achieved using a graduated reference grid. Mice were then IV injected via the tail vein with 25 MBq of ^{99m}Tc-NTP 15-5 simultaneously with the starting of a 90-minute-duration list mode acquisition with a 15% energy window centered on 140 keV. For the analysis of ^{99m}Tc-NTP 15-5 distribution kinetics in mice, acquisition was postprocessed using a 30-second sampling time. Quantitative analysis of scintigraphic scans was performed using *GAMMAVISION+* software (Biospace Mesures). Time activity curves were obtained from regions of interest (ROIs) drawn around the heart (being representative for blood activity), liver, kidneys, bladder, whole knee, and whole body. All measured activities were corrected for radioactive decay. Tracer uptake was expressed as a percentage of the whole-body activity (% WBA). The overall mean for all animals was determined.

Biodistribution Study by Static Planar Imaging

To test cartilage uptake and retention, mice (*n* = 12) were IV injected with 25 MBq of the tracer. At 5, 15, 60, and 90 minutes postinjection, a 5-minute static image was acquired. Animals were positioned over the collimator of the gamma camera, with both femorotibial joints stretched in extension as previously described. Quantitative analysis of scintigraphic scans was performed using *GAMMAVISION+* software. ROIs were drawn around all "visible" organs (ie, the liver, kidneys, and bladder) and around the whole femorotibial joint pattern. A reference region of equal size was placed over the adjacent leg muscle for background evaluation. All activ-

ity values were corrected for radioactive decay, and the overall mean for all animals was determined at each time point. The results were finally expressed as % WBA and compared with decay-corrected activities in explanted organs. For each animal, a cartilage to background ratio (CBR) was also determined at each time point, and the overall mean for all animals was expressed.

Biodistribution Study by Dissection

The animal population used for static imaging was reinjected 7 days later with 25 MBq of the tracer. At the same time points as for imaging (ie, 5, 15, 60, and 90 minutes postinjection), three animals per point were sacrificed (CO_2 inhalation) for a limited biodistribution study. "Nonspecific" organs that have been visualized on static images (ie, kidneys, liver, and bladder) and whole femorotibial joints were removed and their radioactivity was counted using a gamma-counter (Minaxi γ 5530, Packard, Rungis, France). An aliquot of the injected solution was counted simultaneously. After counting, the joints were dissected, and the femoral condyle and tibial plateau were dissociated for (1) 5-minute ex vivo scintigraphy and (2) radioactivity counting. All activity values were corrected for radioactive decay, and for each organ, the overall mean was determined. The results were finally expressed as a percentage of the injected activity (% IA) per organ.

Pinhole SPECT Imaging

In vivo pinhole SPECT acquisition started 10 minutes after IV administration of ^{99m}Tc-NTP 15-5 tracer (80 MBq per animal). Mice (*n* = 6) were positioned on the rotating platform with both femorotibial joints stretched in extension. Reproducibility in joint positioning for the serial images among all animals imaged was achieved using the contention system of the rotating platform. Animals were scanned using the 1 mm pinhole collimator, placed at a radius of rotation of 3 cm.[11] A list mode acquisition, focused on the posterior members of the animals, was performed for 60 minutes, with a 15% energy window centered on 140 keV. Tomographic reconstruction was performed using a validated three-dimensional ordered subset expectation maximization algorithm with three iterations and was visualized using *AMIRA* software (Biospace Mesures), with sections being reconstructed in the three axes of the animals.

For quantitative analysis of scans, fixed ROIs were drawn on five successive coronal sections (0.25 mm thick) over femoral and tibial plateau patterns of the femorotibial joint pattern. The results obtained from five consecutive coronal sections were averaged and expressed as % IA. IA was obtained by scanning a calibrated phantom in the same conditions as animals. The results were compared with decay-corrected gamma counts in dissected tibial plateau and femoral condyle.

Our aim was also to define a relevant criteria for a semiquantitative assessment of tracer accumulation within cartilage that would allow monitoring of joint integrity and functionality over time. Pinhole SPECT acquisition was done three times in each mouse, over a period of 9 days. Quantitative reproducibility of the cartilage signal was determined using ROI-based counts of femoral condyle and tibial plateau, normalized to (1) the injected dose and (2) muscle activity determined from an ROI of equivalent size being placed over the adjacent leg muscle.

Five consecutive coronal planes were averaged and analyzed in each approach, and the reproducibility over the scans was compared by averaging the calculated coefficient of variation CV = (SD/mean) × 100.

Results

Kinetics of Tracer Distribution in Mice and Scintigraphic Imaging of Cartilage

Representative DPIs of ^{99m}Tc-NTP 15-5 uptake in healthy mice and overall mean time activity curves of organs are displayed in Figure 2 and Figure 3, respectively. ^{99m}Tc-NTP 15-5 was rapidly distributed in organs, with a nonspecific accumulation being evidenced in the kidneys and the liver as early as the first minutes after administration. ^{99m}Tc-NTP 15-5 rapidly cleared from the blood in a one-exponent fashion, as shown in Figure 3A. The high level of radioactivity in kidneys and the substantial accumulation of radioactivity within the bladder from 20 minutes postinjection indicated a major rapid urine route of excretion.

For the femorotibial joint, the peak of radioactivity was reached within 5 minutes and was maintained for at least 90 minutes postinjection to an overall mean activity of 0.4% WBA for each femorotibial joint (see Figure 3C). No drop was observed in the joint activity in decay-corrected time activity curves during the 90-minute postinjection period.

^{99m}Tc-NTP 15-5 uptake in the joint was high respective to background, with an overall mean CBR
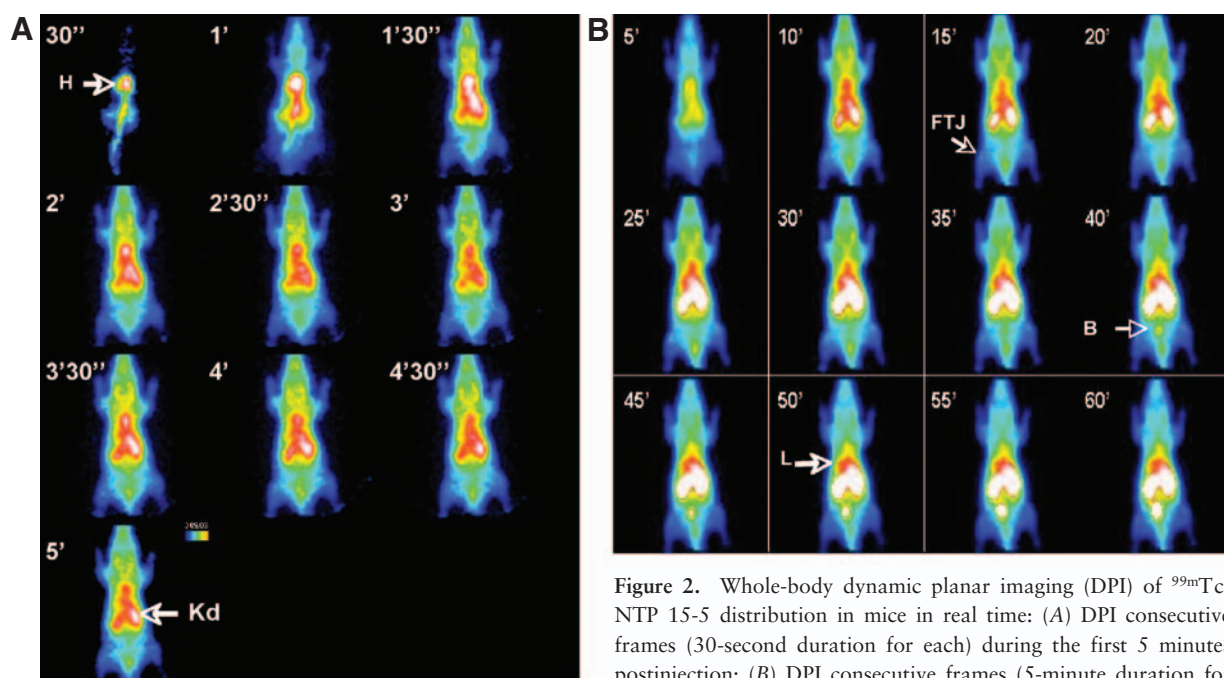

Figure 2. Whole-body dynamic planar imaging (DPI) of ^{99m}Tc-NTP 15-5 distribution in mice in real time: (*A*) DPI consecutive frames (30-second duration for each) during the first 5 minutes postinjection; (*B*) DPI consecutive frames (5-minute duration for each) during the period of 5 to 60 minutes. B = bladder; FTJ = femorotibial joint; H = heart; Kd = kidney; L = liver.
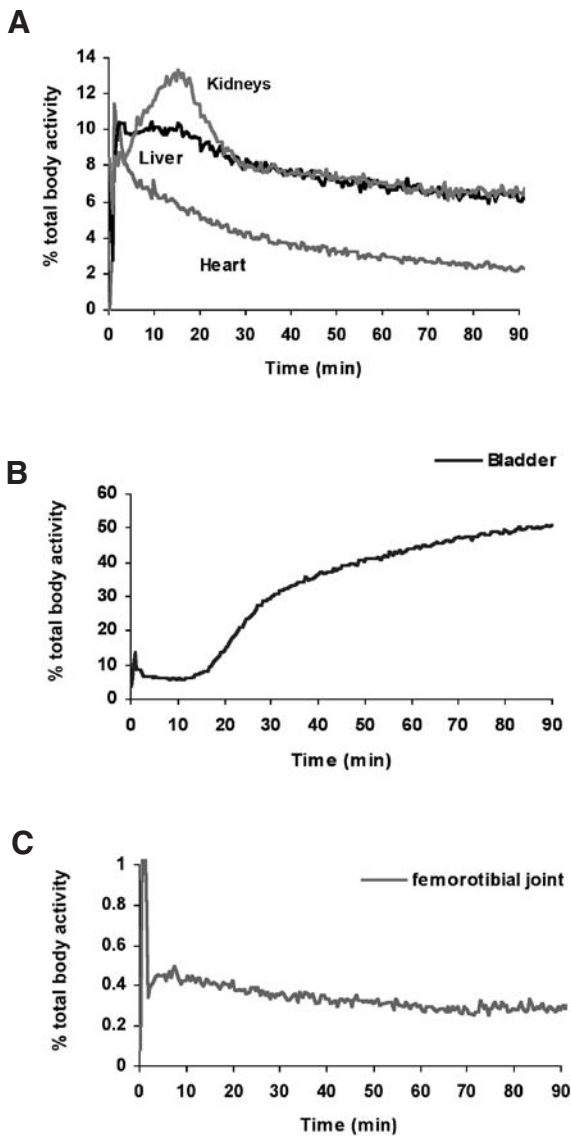
Figure 3. Time activity curves for ^{99m}Tc-NTP 15-5 distribution in vivo after intravenous injection in mice: time activity curves for (*A*) nonspecific organs: heart, liver, and kidneys; (*B*) the bladder; (*C*) and the whole femorotibial joint. Mean values are presented.

of 2.5 ± 0.3, thus leading to high-contrast joint imaging being obtained as early as 15 minutes postinjection, even in planar projection. As evidenced in Figure 4A, the radioactivity uptake of tibial plateau cartilage could be considered as being discernible from that of femoral condyle cartilage. In vivo cartilage imaging was confirmed by ex vivo imaging of the dissected femorotibial joint that localized a high accumulation of radioactivity within cartilaginous structures with an absence of radiotracer accumulation within bone (Figure 4, G and H).

When 1 mm pinhole SPECT acquisition was performed, tibial plateau cartilage uptake was clearly delineated from that of femoral condyle: medial and lateral compartments of both the femoral condyle and the tibial plateau were highly imaged and delineated on both the three-dimensional volume and associated coronal and axial slices (Figure 4, B and D–F). The interarticular space that did not concentrate ^{99m}Tc-NTP 15-5 was also clearly delineated from cartilage tissue, both by the three-dimensional reconstructed volume and the 0.25 mm–thick sagittal slice of the knee.

Quantitative Analysis of ^{99m}Tc-NTP 15-5 Scintigraphic Imaging

Tracer was observed to accumulate within liver with a mean uptake value of 8.0 ± 0.9% WBA from 5 to 90 minutes postinjection. Tracer accumulation within kidneys ranged between 7.8 ± 1.6% (for each kidney) at 5 minutes postinjection and 5.8 ± 0.7% WBA at 90 minutes postinjection. The bladder showed an increased accumulation of the tracer from 5 minutes postinjection (4.0 ± 1.9% WBA) to 90 minutes postinjection (50.6 ± 11. 4% WBA) (Figure 5A). For the articular cartilage target, tracer uptake within the whole femorotibial joint was evaluated by planar imaging as ranging between 0.5 ± 0.1% WBA at 5 minutes postinjection and 0.4 ± 0.11% WBA at 90 minutes postinjection (Figure 5B). Given that animals were anesthetized for imaging, no urinary excretion occurred, and whole-body activity could be considered as IA and could be compared with dissection values. A good correlation was found between uptake values determined by ROI analysis and dissection (R^2 = .97). Even if a femoral pattern could be discernible from a tibial pattern on planar scans, it was difficult to delineate separate ROIs for a separate quantitation. Separate quantitation of ^{99m}Tc-NTP 15-5 accumulation was performed on SPECT coronal planes and led to uptake values of 0.17 ± 0.04% IA and 0.21 ± 0.0 3% IA for the femoral condyle and tibial plateau, respectively. Dissection values obtained at 90 minutes postinjection (*n* = 3 animals) were 0.15 ± 0.09% IA and 0.21 ± 0.03% IA for the femoral condyle and tibial plateau, respectively.

Reproducibility of Semiquantitative Analysis of Cartilage Signal

Reproducibility of the cartilage signal quantitation was determined using ROI-based counts of the
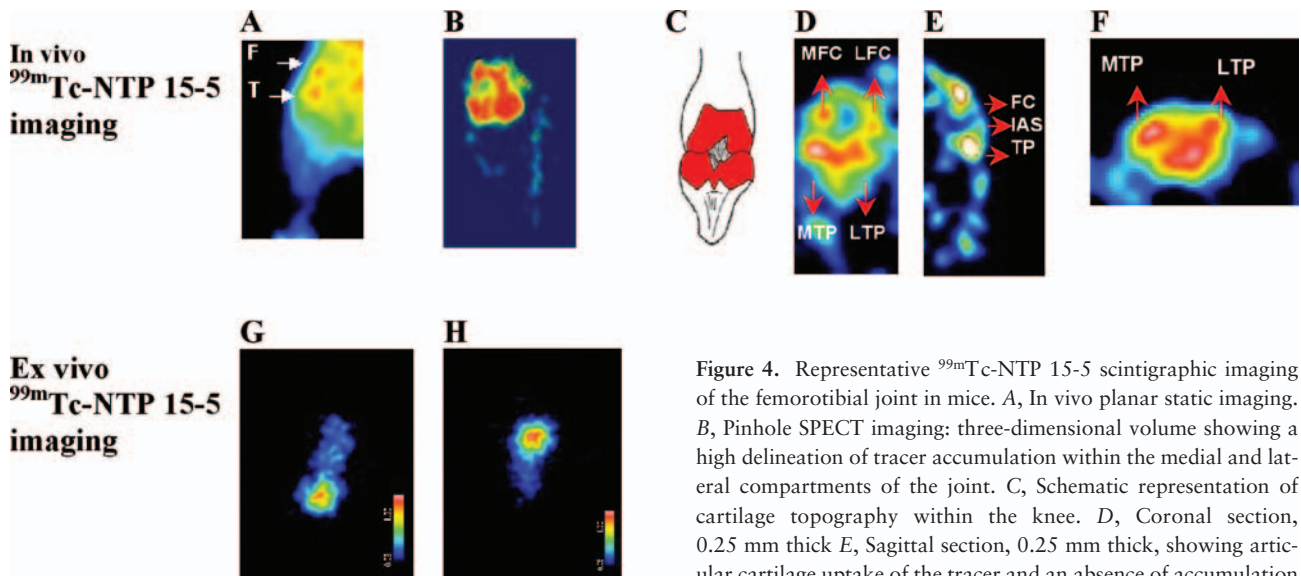
Figure 4. Representative ^{99m}Tc-NTP 15-5 scintigraphic imaging of the femorotibial joint in mice. *A*, In vivo planar static imaging. *B*, Pinhole SPECT imaging: three-dimensional volume showing a high delineation of tracer accumulation within the medial and lateral compartments of the joint. *C*, Schematic representation of cartilage topography within the knee. *D*, Coronal section, 0.25 mm thick *E*, Sagittal section, 0.25 mm thick, showing articular cartilage uptake of the tracer and an absence of accumulation within the interarticular space. *F*, Axial section, 0.25 mm thick. *G*, Ex vivo scintigraphy of a dissected femur. *H*, Ex vivo scintigraphy of dissected tibia. F = femoral condyle cartilage uptake; FC = femoral condyle; IAS = interarticular space; LFC = lateral femoral condyle; LTP = lateral tibial plateau; MFC = medial femoral condyle; MTP = medial tibial plateau; T = tibial plateau cartilage uptake; TP = tibial plateau.

femoral condyle and tibial plateau, normalized to (1) the injected dose and (2) muscle activity. The results are presented in Table 1. With both semiquantitative approaches, the % CV between scans was lower than 20%. The highest reproducibility was achieved by normalizing the cartilage signal to an equivalent ROI over the muscle, with an average % CV across successive scans being 11.7 ± 4.9% and 11.2 ± 4.6% for the femoral condyle and tibial plateau, respectively.

Discussion

The purpose of this article was to report a new imaging approach for the in vivo functional assessment of cartilage in small animals using ^{99m}Tc-NTP 15-5. On the basis of previous results illustrating the relevance of this tracer for scintigraphic imaging of cartilage, we hypothesized that the ^{99m}Tc-NTP 15-5 tracer would be a powerful tool to assess cartilage integrity in mice models, which has great potential for OA research.[7–10,18,19] As a first step toward a scintigraphic study using a new animal species, the distribution of ^{99m}Tc-NTP 15-5 was investigated in the mouse by both

DPI and tissue counting: As expected from previous animal studies, the peak of radioactivity was reached within the articular cartilage of the mouse knee from 5 minutes postinjection and was maintained for at least 90 minutes postinjection.[18,19] Tracer kinetics was thus compatible with a 60-minute duration pinhole SPECT acquisition. A good correlation was found between tracer uptake values determined by ROI analysis and dissection. Given that bone and muscle did not show any accumulation of the tracer, an overall mean CBR of 2.5 ± 0.3 (obtained as early as 15 minutes postinjection) led to a contrasted joint imaging, even in planar projection conditions. Visual inspection of planar scans revealed that a tibial plateau cartilage pattern was discernible from that of femoral condyle. Using planar images, an accurate ROI delineation over each component of the femorotibial joint (for a separate quantitation) was difficult. Separate quantitation was easily feasible using pinhole SPECT acquisition and allowed topographic localization of ^{99m}Tc-NTP 15-5 tracer distribution in vivo within the femorotibial joint. The medial and lateral compartments of both the femoral condyle and the tibial plateau were imaged and delineated on both the three-dimensional volume and asso-
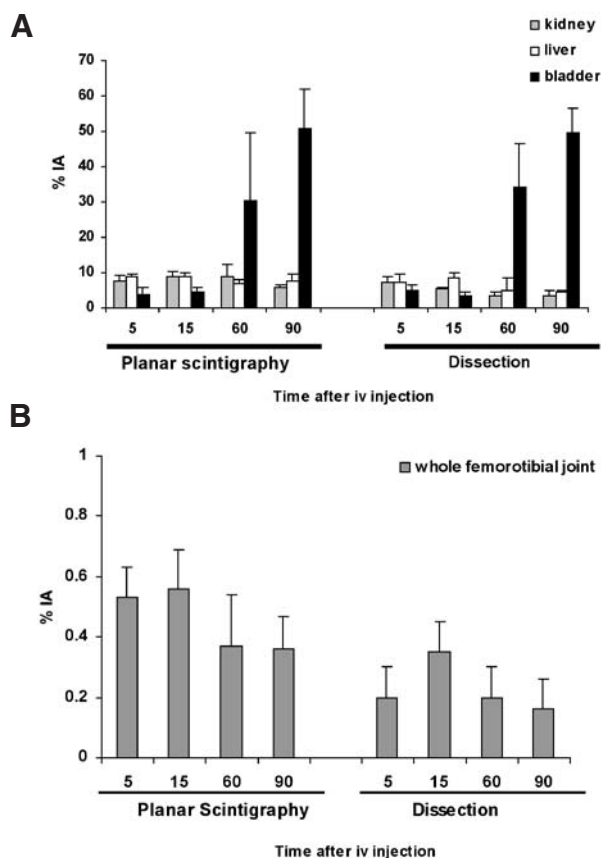
Figure 5. The results of a ^{99m}Tc-NTP 15-5 biodistribution study being performed by both in vivo planar static imaging and dissection: biodistribution within (*A*) nonspecific organs: heart liver, kidneys and (*B*) the whole femorotibial joint. Mean percentage of injected activity (% IA) is given with standard deviation.

ciated coronal and axial slices. These in vivo SPECT images were consistent with those of our previously published study, which demonstrated (by autoradiographic analysis of radioactivity distribution within the femorotibial joint of guinea pigs) that ^{99m}Tc-NTP 15-5 accumulation could be closely related to the topography of articular cartilage.[19] Given that our objective was to evaluate the feasibility of ^{99m}Tc-NTP

15-5 imaging for its ability to stage cartilage integrity in a quantitative manner in the same animals over time, it appeared essential to define the most reproducible method for quantitative analysis of cartilage signal. Reproducibility of cartilage signal quantitation was determined using ROI-based counts of femoral condyle and tibial plateau, normalized to (1) the injected dose and (2) muscle. The lowest variation (CV = 11.7 ± 4.9% for femoral uptake and 11.2 ± 4.6% for tibial uptake over the subsequent scans) was obtained by normalizing cartilage activity to muscle activity. A good correlation was found between tracer uptake values determined by ROI analysis of pinhole SPECT acquisitions and dissection.

To our knowledge, this is the first time that small-animal radionuclide imaging of cartilage in vivo has been reported in mice by using ^{99m}Tc-NTP 15-5 radiotracer. To date, radiotracers currently available for OA provide only indirect evaluations of the pathology, such as bone remodeling and inflammation. However, they do not seem specific enough to evaluate disease progression and the response to therapy in both preclinical and clinical studies.[20,21] Preliminary animal studies have underlined the potential of radiolabeled molecules interacting with constituents of the ECM, or antikeratan sulfate monoclonal antibodies, for a specific targeted imaging of cartilage.[22,23] However, the specificity of these agents, their level of accumulation within cartilage tissues, and the radionuclide are not yet optimal for routine preclinical use. From our work, ^{99m}Tc-NTP 15-5 scintigraphy of cartilage appears to be easily applicable for routine preclinical use in mouse models. According to us, this study responded to a major challenge in radionuclide imaging, which was the size of cartilage structures in the mouse (femoral condyle and tibial plateau being less than 5 mm across). Nevertheless, these experimental results in healthy mice raised the question of whether ^{99m}Tc-NTP 15-5 imaging would be sufficiently sensitive for

Table 1 Reproducibility of Cartilage Signal Semiquantification over Three Scans in Six Mice Using Two Normalization Approaches

	% CV ± SD	
Normalization Approach	*Femoral Cartilage Uptake*	*Tibial Cartilage Uptake*
Injected dose	13.6 ± 3.7	15.7 ± 5.4
Muscle	11.7 ± 4.9	11.2 ± 4.6

CV = coefficient of variation.

in vivo assessment of OA cartilage in experimental models. The potential of ^{99m}Tc-NTP 15-5 scintigraphy to detect cartilage alterations at an early stage and track progressive articular degeneration in vivo was previously demonstrated in small-animal models of OA: in the meniscectomized guinea pig model of OA, ^{99m}Tc-NTP 15-5 scintigraphy was demonstrated to be highly sensitive for quantifying in vivo PG content changes associated with both hypertrophic and decompensation responses of pathologic cartilage.[19] By comparing both scintigraphic and autoradiographic patterns of tracer accumulation in the OA knees of guinea pigs, we previously showed that radioactivity defects of less than 4 mm in diameter at the medial compartment of the femorotibial joint affected the in vivo imaging in a robust fashion.[19] Such radionuclide PG imaging of a biomechanical OA model appeared to be particularly sensitive since ^{99m}Tc-MDP bone scintigraphy failed to detect any changes throughout the study. As a consequence, we hypothesize that the high sensitivity of ^{99m}Tc-NTP 15-5 imaging to PG content should allow the assessment of early ECM alterations in vivo in transgenic models. Indeed, mouse strains with spontaneous or engineered genetic alterations in collagene (Cho/+ and Dmm/+ mice), aggrecan gene (Cmd/+ mice), cartilage matrix (Cmd/+ mice), and matrix metalloproteinase 13 expressions have created a great demand for studying and characterizing the role of these extra- and intracellular pathways in the initiation and progression of cartilage lesions.[7,24,25]

In light of these encouraging results in healthy mice, we now intend to evaluate the relevance of ^{99m}Tc-NTP 15-5 imaging compared with other functional agents (ie, bone remodeling and inflammation agents) for characterizing in vivo mouse strains with engineered genetic alterations of ECM components and evaluating DMOAD efficacy. Moreover, considering that ^{99m}Tc-NTP 15-5 radiotracer is currently under validation for clinical application in humans, this experimental imaging approach may represent the opportunity to bridge the gap between preclinical and clinical testing.

Acknowledgment

References

1. Buckwalter JA, Martin JA. Osteoarthritis. Adv Drug Deliv Rev 2006;58:150–67.
2. Krasnokutsky S, Samuels J, Abramson B. Osteoarthritis in 2007. Bull NYU Hosp Jt Dis 2007;65:222–8.
3. Yelin Y. The economics of osteoarthritis. In: Brandt KD et al, editors. New York. Oxford University Press; 2003. p. 17–21.
4. Aigner T, McKenna L. Molecular pathology and pathobiology of osteoarthritic cartilage. Cell Mol Life Sci 2002;59:5–18.
5. Pelletier JP, Martel-Pelletier J, Howell DS. Etiopathogenesis of osteoarthritis. In: Koopman WJ, editor. Arthritis & allied conditions. A textbook of rheumatology. Baltimore: Williams & Wilkins; 2001. p. 2195–45.
6. Aigner T, Sachse A, Gebhard PM, Roach HI. Osteoarthritis: pathobiology-targets and ways for therapeutic intervention. Adv Drug Deliv Rev 2006;58:128–49.
7. Glasson SS. In vivo osteoarthritis target validation utilizing genetically-modified mice. Curr Drug Targets 2007;8:367–76.
8. Jouzeau JY, Gillet P, Netter P. Interest of animal models in the preclinical screening of anti-osteoarthritic drugs. Joint Bone Spine 2000;67:565–9.
9. Helminen HJ, Säämänen AM, Salminen H, Hyttinen MM. Transgenic mouse models for studying the role of cartilage macromolecules in osteoarthritis. Rheumatology 2002;41:848–56.
10. Young MF. Mouse models of osteoarthritis provide new research tools. Trends Pharmacol Sci 2005;26:333–5.
11. Weissleder R, Mahmood U. Molecular imaging. Radiology 2001;219:316–33.
12. Gillies RJ. In vivo molecular imaging. J Cell Biochem Suppl 2002;39:231–8.
13. Meikle SR, Kench P, Kassiou M, Banati RB. Small animal SPECT and its place in the matrix of molecular imaging technologies. Phys Med Biol 2005;50:R45–61.
14. Beekman F, Van Der Have F. The pinhole: gateway to ultra-high-resolution three-dimensional radionuclide imaging. Eur J Nucl Med Mol Imaging 2007;34:151–61.
15. Mayer-Kuckuk P, Boskey AL. Molecular imaging promotes progress in orthopedic research. Bone 2006;39:965–77.
16. Madelmont JC, Giraud I, Nicolas C, et al, inventors. Novel quaternary ammonium derivatives, method for preparing same and pharmaceutical use. Patent 99,08020. 1999.
17. Nicolas C, Borel M, Maurizis JC, et al. Synthesis of N-quaternary ammonium [^{3}H] and [^{99m}Tc] polyazamacrocycles, potential radiotracers for cartilage imaging. J Labelled Cpd Radiopharm 2000;43:585–94.
18. Ollier M, Maurizis JC, Nicolas C, et al. Joint scintigraphy in rabbits with ^{99m}Tc-N-[3-(triethylammonio)propyl]-

15ane-N5, a new radiodiagnostic agent for articular cartilage imaging. J Nucl Med 2001;42:141–5.

19. Miot-Noirault E, Vidal A, Pastoureau P, et al. Early detection and monitoring of cartilage alteration in the experimental meniscectomized guinea pig of osteoarthritis by ^{99m}Tc-NTP 15-5 scintigraphy. Eur J Nucl Med Mol Imaging 2007;34:1280–90.

20. Mazzuca SA, Brandt KD, Schauwecker DS, et al. Bone scintigraphy is not a better predictor of progression of knee osteoarthritis than Kellgren and Lawrence grade. J Rheumatol 2004;31:329–32.

21. Nakamura H, Masuko K, Yudoh K, et al. Positron emission tomography with ^{18}F-FDG in osteoarthritic knee. Osteoarthritis Cartilage 2007;15:673–81.

22. Yu SW, Shaw SM, Van Sickle DC. Radionuclide studies of articular cartilage in the early diagnosis of arthritis in the rabbit. Ann Acad Med Singapore 1999;28:44–8.

23. Kairemo KJA, Lappalainen AK, Kaapa E, et al. In vivo detection of intervertebral disk injury using a radiolabeled monoclonal antibody against keratan sulfate. J Nucl Med 2001;42:476–82.

24. Aszodi A, Pfeifer A, Wendel M, et al. Mouse models for extracellular matrix diseases. J Mol Med 1998; 76:238–52.

25. Neuhold LA, Killar L, Zhao W, et al. Postnatal expression in hyaline cartilage of constitutively active human collagenase-3 (MMP-13) induces osteoarthritis in mice. J Clin Invest 2001;107:35–44.